

## Structural, magnetic, thermal, and transport properties of $X_8\text{Ga}_{16}\text{Ge}_{30}$ ( $X = \text{Eu}, \text{Sr}, \text{Ba}$ ) single crystals

B. C. Sales, B. C. Chakoumakos, R. Jin, J. R. Thompson, and D. Mandrus

*Solid State Division, Oak Ridge National Laboratory Oak Ridge, Tennessee 37831-6056*

(Received 26 December 2000; revised manuscript received 15 March 2001; published 6 June 2001)

Structural, magnetic, electrical and thermal transport, and heat-capacity measurements are reported on single crystals of  $\text{Eu}_8\text{Ga}_{16}\text{Ge}_{30}$ ,  $\text{Sr}_8\text{Ga}_{16}\text{Ge}_{30}$ , and  $\text{Ba}_8\text{Ga}_{16}\text{Ge}_{30}$ . These compounds all crystallize in a cubic type-I ice clathrate structure, and are of interest as potential thermoelectric materials. Neutron-diffraction measurements were made on a single crystal of  $\text{Eu}_8\text{Ga}_{16}\text{Ge}_{30}$  that was grown using isotopically pure  $\text{Eu}^{153}$ . Nuclear density maps clearly show that Eu atoms at the  $6d$  sites  $(\frac{1}{4}, \frac{1}{2}, 0)$  can move away from the cage center to one of four nearby positions. Ferromagnetism is observed in  $\text{Eu}_8\text{Ga}_{16}\text{Ge}_{30}$  for temperatures below 32 K, with the preferred direction of the Eu spins along the (100) axis. Ferromagnetism in these heavily doped semiconductors ( $\approx 10^{21}$  electrons/cm<sup>3</sup>) is likely due to a Rudermann-Kittel-Kasuya-Yoshida-type interaction. A large ( $\approx 10\%$  at 8 T) negative magnetoresistance was measured near the Curie temperature of  $\text{Eu}_8\text{Ga}_{16}\text{Ge}_{30}$ . The lattice thermal conductivities of  $\text{Eu}_8\text{Ga}_{16}\text{Ge}_{30}$  and  $\text{Sr}_8\text{Ga}_{16}\text{Ge}_{30}$  single crystals show all of the characteristics of a structural glass. The thermal conductivity of  $\text{Ba}_8\text{Ga}_{16}\text{Ge}_{30}$  is low at room temperature (1.3 W/m K), but exhibits a temperature dependence characteristic of a crystal. A magnetic field has no significant effect on the thermal conductivity of any of the crystals for temperatures between 2 and 300 K. Heat-capacity measurements indicated Einstein contributions from each of the rattlers, with characteristic temperatures of 60, 53, and 30 K for Ba, Sr, and Eu atoms respectively. No superconductivity was observed in heavily doped single crystals of  $\text{Ba}_8\text{Ga}_{16}\text{Ge}_{30}$  for temperatures above 2 K, contrary to a previous report.

DOI: 10.1103/PhysRevB.63.245113

PACS number(s): 72.15.Jf, 61.12.-q, 75.30.-m

### I. INTRODUCTION

One of the more interesting ideas in the area of thermoelectric materials research is the concept of designing a solid that conducts heat like a glass but maintains the good electrical properties associated with crystals.<sup>1</sup> The essence of this idea is to synthesize semiconducting compounds in which one of the atom types is weakly bound in an oversized atomic cage. Such an atom will undergo large localized vibrations, and will be referred to as a ‘‘rattler.’’ If the characteristic vibration frequency of the rattler is low enough, the rattler can resonantly scatter the acoustic phonons that carry most of the heat in a crystal, which can result in a crystal with a very low lattice thermal conductivity. If most of the electronic conduction takes place via the framework atoms (i.e., electronic bands associated primarily with the atoms that form the cages), then a good thermoelectric material can result. The validity of this concept was first demonstrated in a class of cubic compounds known as filled skutterudites, that were shown to have superior thermoelectric properties in the 700–1000-K temperature range.<sup>2–5</sup>

The thermal conductivity of glasses,  $\kappa$ , is not only very small,<sup>6,7</sup> but displays a universal temperature dependence:  $\kappa$  varies as  $T^2$  below 1 K, has a plateau in the region from 10 to 20 K, and is roughly independent of temperature above 100 K. This behavior is qualitatively different from ordinary crystalline behavior, in which  $\kappa$  reaches a maximum between 20 and 50 K, and shows no plateau. Although filled skutterudites exhibit a low lattice thermal conductivity, the temperature dependence of  $\kappa$  is still characteristic of a crystalline solid.<sup>4</sup>

Recently Nolas and co-workers<sup>8,9</sup> reported a cubic crys-

talline semiconductor  $\text{Sr}_8\text{Ga}_{16}\text{Ge}_{30}$  with good electronic properties, but with a lattice thermal conductivity that exhibited all of the characteristics of a structural glass. A large number of similar semiconducting compounds<sup>10–12</sup> with the same cubic structure are isotypic with a type-I ice clathrate. The structural simplicity of the semiconducting clathrates makes them ideal candidates to study the microscopic origin of glasslike heat conduction in a crystalline solid. We are particularly interested in understanding why certain rattlers produce a glasslike thermal conductivity, while others only lower the thermal conductivity. In the present paper we focus on the properties of three crystalline semiconductors all with the same cubic clathrate crystal structure:  $\text{Eu}_8\text{Ga}_{16}\text{Ge}_{30}$ ,  $\text{Sr}_8\text{Ga}_{16}\text{Ge}_{30}$ , and  $\text{Ba}_8\text{Ga}_{16}\text{Ge}_{30}$ . The Eu rattler is of particular interest, because it carries a large magnetic moment that can be probed using an external magnetic field.

### II. EXPERIMENTAL METHODS

#### A. Crystal growth

Large (1 cm<sup>3</sup>) single crystals of  $\text{Eu}_8\text{Ga}_{16}\text{Ge}_{30}$ ,  $\text{Sr}_8\text{Ga}_{16}\text{Ge}_{30}$ , and  $\text{Ba}_8\text{Ga}_{16}\text{Ge}_{30}$  were grown by slowly cooling (1–2 °C/h) molten stoichiometric mixtures of the elements in carbon-coated evacuated silica tubes. When the temperature attained a value some 50–70 °C below the melting point, the cooling was stopped for 3–5 days before cooling to room temperature at 2 °C/min. The measured melting points of  $\text{Eu}_8\text{Ga}_{16}\text{Ge}_{30}$ ,  $\text{Sr}_8\text{Ga}_{16}\text{Ge}_{30}$ , and  $\text{Ba}_8\text{Ga}_{16}\text{Ge}_{30}$  were  $688 \pm 5$ ,  $770 \pm 5$ , and  $963 \pm 5$  °C, respectively, as determined by differential thermal analysis. The melting points for the Sr and Ba compounds are in good agreement with the values reported previously.<sup>10,13</sup> For the Ba and Sr compounds, el-

elemental Ba (99.9% Alfa Aesar) and Sr (99.95% Alfa Aesar) pieces were first arc melted together in an argon atmosphere with Ge [99.9999% zone-refined rods from Oak Ridge National Laboratory (ORNL)] pieces to form  $\text{BaGe}_2$  or  $\text{SrGe}_2$ . The exact compositions of the binary compounds were determined from the weight losses, assuming that only Ba or Sr was lost as vapor. The prereacted  $\text{BaGe}_2$  and  $\text{SrGe}_2$  solids were somewhat air sensitive, and hence were weighed and handled in an inert atmosphere. Appropriate amounts of Ge and Ga were arc melted together with the binary compounds to form polycrystalline  $\text{Sr}_8\text{Ga}_{16}\text{Ge}_{30}$ , and  $\text{Ba}_8\text{Ga}_{16}\text{Ge}_{30}$ . Polycrystalline  $\text{Eu}_8\text{Ga}_{16}\text{Ge}_{30}$  could be prepared in a way similar to the Sr and Ba compounds, but it was also possible to directly arc melt Eu metal ingots (99.99%, Ames Laboratory) together with appropriate amounts of Ge and Ga to form polycrystalline  $\text{Eu}_8\text{Ga}_{16}\text{Ge}_{30}$ . Once the ternary clathrate phases were formed, they were stable in air. The polycrystalline material was loaded into a carbon-coated silica tube, and thermally processed into a single crystal as described above. For the single-crystal neutron experiments, isotopically pure  $^{153}\text{Eu}$  was used in the synthesis, rather than natural Eu which strongly absorbs neutrons. For the neutron-scattering, magnetic-susceptibility, heat-capacity, and thermal and electrical transport measurements, single crystals were cut to the appropriate size using a low-speed diamond saw. Polished faces of the single crystals were examined using energy-dispersive x-ray diffraction, optical microscopy, Laue x-ray back-reflection, and neutron transmission to ensure that the crystals were homogeneous and of the appropriate 8-16-30 composition. Since these clathrates have a cubic crystal structure, there was no attempt in the present experiments to measure transport properties along specific crystallographic directions.

Several polycrystalline samples of  $\text{Eu}_8\text{Ga}_{16}\text{Ge}_{30}$  were annealed in a dynamic vacuum of about  $1 \times 10^{-6}$  torr at 550 °C for five days, in an attempt to improve the crystallinity and lower the carrier concentration, which was typically about  $10^{21}$  electron/cm<sup>3</sup> in as-prepared polycrystalline samples. After annealing, however, a completely different crystal structure was obtained. This structure is isomorphic with another cubic clathrate phase  $\text{Ba}_8\text{Ga}_{16}\text{Sn}_{30}$ , first reported in Ref. 10. The  $\text{Eu}_8\text{Ga}_{16}\text{Ge}_{30}$  clathrate phase has a space group of  $I-43m$  (No. 217) and a lattice constant of 10.62 Å. The properties of this phase will be reported elsewhere.

### B. Measurements

Powder x-ray-diffraction measurements were made using Cu  $K\alpha$  radiation and a commercial SCINTAG diffractometer equipped with a nitrogen cooled Ge detector. Real-time x-ray Laue measurements were made using a commercial system from Multiwire Laboratories Ltd. Single-crystal neutron-diffraction experiments from 10 to 295 K were conducted at ORNL's High Flux Isotope Reactor using a four-circle neutron diffractometer and a closed-cycle liquid-helium refrigerator.<sup>14</sup> Chemical composition information was obtained directly using a Princeton Gamma Tech energy dispersive x-ray system and an International Scientific Instruments scanning electron microscope. Metallographic

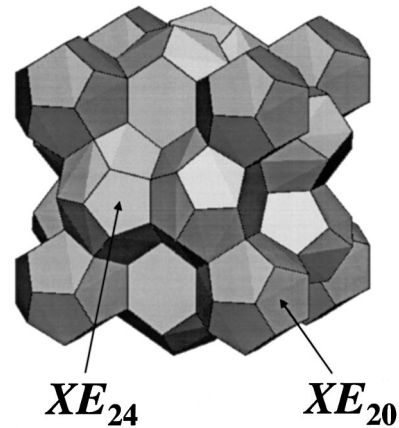


FIG. 1. Models of the  $\text{Eu}_8\text{Ga}_{16}\text{Ge}_{30}$ ,  $\text{Sr}_8\text{Ga}_{16}\text{Ge}_{30}$ , and  $\text{Ba}_8\text{Ga}_{16}\text{Ge}_{30}$  crystal structures. The cubic crystal structure is composed of two types of polyhedra that consist of either 20 or 24 vertices ( $\text{XE}_{24}$  or  $\text{XE}_{20}$ ). Gallium and germanium atoms are randomly distributed among all of the vertices. The Sr, Ba, or Eu atoms are located at the center of each polyhedral cage. The space group is  $Pm-3n$  with a typical lattice constant of about 10.7 Å. This structure is isotypic, with a type-I ice clathrate structure.

investigations were performed on polished surfaces using standard optical microscopy techniques. Magnetic susceptibility and magnetization measurements were made from 5 to 300 K in applied fields from 0.001 to 6.5 T using a commercial superconducting quantum interference device magnetometer from Quantum Design. Electrical and thermal transport data from 10 to 300 K were obtained using a closed-cycle helium refrigerator system described in detail elsewhere.<sup>4</sup> Resistivity, Hall, and ac susceptibility measurements were made in a commercial physical property measurement system (PPMS) from Quantum Design. Hall data were taken using the standard Hall geometry and a sample rotator that reversed the direction of the field with respect to the sample. In addition, thermal conductivity and Seebeck measurements were made from 2 to 300 K with a thermal transport option (TTO) for the PPMS from Quantum Design. Cyclic heat pulses were applied to the sample, while the temperature gradient was monitored by two thin film Cernox chip thermometers. The data was fit in real time to a dual time-constant model using a nonlinear least-squares technique. There was excellent agreement between the thermal conductivity and Seebeck data obtained with the home-built closed-cycle refrigerator system and the data obtained with the TTO for the PPMS.

## III. RESULTS AND DISCUSSION

### A. Crystallography, “rattling,” and tunneling

The compounds  $\text{Eu}_8\text{Ga}_{16}\text{Ge}_{30}$ ,  $\text{Sr}_8\text{Ga}_{16}\text{Ge}_{30}$ , and  $\text{Ba}_8\text{Ga}_{16}\text{Ge}_{30}$  crystallize in the same cubic crystal structure, space group  $Pm-3n$ , and are isotypic with the type-I hydrate structure  $X_8(\text{H}_2\text{O})_{46}$  of the ice clathrate.<sup>10,14,15</sup> (Fig. 1) This crystal structure consists of two types of large polyhedral cages consisting of 24 and 20 vertices, respectively. A Ge or Ga atom randomly occupies each of the vertices.<sup>14</sup> The alkaline earth or Eu atoms reside at or near the center of each

cage. If these compounds are treated as Zintl phases,<sup>16</sup> it is easy to rationalize why they should be semiconductors. Each Ge is covalently bonded to four other Ge or Ga atoms. This is similar to the bonding found in elemental Ge. Ga has one less bonding electron than Ge, which is formally compensated by the two electrons per atom, donated by Eu, Sr, or Ba. In the Zintl concept, the strongly electropositive cations (Eu, Ba, and Sr) simply provide the necessary charge to complete the outer electron shells of the Ge and Ga anions.<sup>10</sup> This simple picture is consistent with experimental results on lightly doped  $\text{Sr}_8\text{Ga}_{16}\text{Ge}_{30}$  and  $\text{Ba}_8\text{Ga}_{16}\text{Sr}_{30}$ ,<sup>8,13</sup> as well as detailed calculations of the electronic structure.<sup>17,18</sup>

The room-temperature lattice constants of the three compounds are similar: 10.70 Å ( $\text{Eu}_8\text{Ga}_{16}\text{Ge}_{30}$ ), 10.72 Å ( $\text{Sr}_8\text{Ga}_{16}\text{Ge}_{30}$ ), and 10.78 Å ( $\text{Ba}_8\text{Ga}_{16}\text{Ge}_{30}$ ). The typical effective ionic radii for Eu, Sr, and Ba in a high coordination environment are 1.35, 1.44, and 1.60 Å, respectively, which would suggest a much larger change in the clathrate lattice constant. The small variation in lattice constant attests to the weak bonding between the caged atoms and framework atoms of the host. This is particularly true for the cations (Ba, Eu, or Sr) that reside in the larger of the two types of cages with 24 vertices. Single-crystal neutron structure refinements from room temperature to 10 K indicate no change in crystal structure or space group other than a shift in the lattice constant due to normal thermal contraction with decreasing temperature.<sup>14</sup>

One of our principal interests in these compounds is the connection between atomic displacement parameters (ADP's) and the lattice thermal conductivity. For several classes of thermoelectric compounds that contain weakly bound atoms (rattlers), it is possible to estimate the lattice thermal conductivity, Debye temperature, and Einstein temperature of the rattler from room-temperature crystallography data.<sup>19,20</sup> For the three clathrate compounds discussed in the present paper, however, this analysis does not work very well, and becomes increasingly poor for the smaller cations (Sr and Eu). The ability of the Sr and Eu atoms to move away from the cage center to one of four nearby sites (consistent with the space group)<sup>14</sup> produces a large component to the ADP parameter that only weakly depends on temperature (Fig. 2). It is not clear if this weakly temperature-dependent value of the mean-square displacement (ADP value) is due to the static displacement of the Eu or Sr atoms to one of the four nearby sites, or to motion between the four sites with a small activation barrier. If some dynamic motion occurs between the four sites, however, it is not obvious how to analyze the ADP data.

Single-crystal neutron-diffraction data were used to determine the nuclear density at the center of the large cage ( $6d$  site,  $\frac{1}{4}, \frac{1}{2}, 0$ ) for the Ba and Sr clathrates at 15 K and the Eu clathrate at 40 K. The data were generated using a difference Fourier map in which the Ba, Sr, or Eu atoms at this site were removed from the structural model (Fig. 3). The nuclear density gives the probability of finding the Ba, Sr, or Eu nucleus at different positions near the center of the cage. The Ba nuclear density is broad, but centered at the center of the cage. Combined with the temperature dependence of the ADP values (Fig. 2), these data suggest that the Ba atoms in

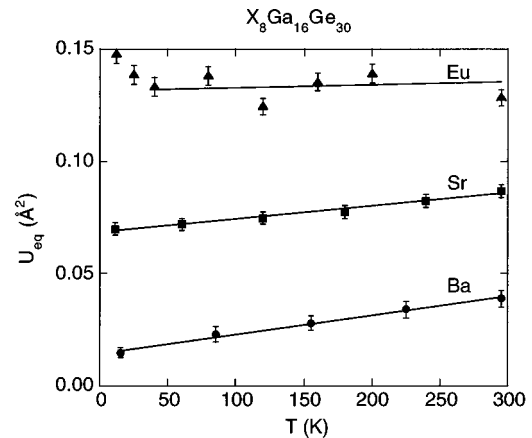


FIG. 2. Isotropic atomic displacement parameters  $U_{eq}$  for Eu, Sr, and Ba atoms at the center of the larger polyhedral cages ( $XE_{24}$ ; see Fig. 1) as determined by single-crystal neutron structure refinements at each temperature.  $U_{eq}$  measures the average mean-square displacement of the atom about a crystallographic position at the center of the cage ( $6d$  site:  $\frac{1}{4}, \frac{1}{2}, 0$ ), averaged over all directions.

this cage can be treated as Einstein oscillators with an Einstein temperature of about 64 K. This value is consistent with fits to the low-temperature heat-capacity data of  $\text{Ba}_8\text{Ga}_{16}\text{Ge}_{30}$ , which give an Einstein temperature for the Ba of 60 K. The Ba atoms appear to behave as normal rattlers similar to the La, Ce, Yb, and Tl atoms in the skutterudites,<sup>4,21,22</sup> or the Tl atoms in  $\text{Tl}_2\text{SnTe}_5$ .<sup>22,23</sup>

The Sr nuclear density is even broader than that for the Ba atoms (Fig. 3), and indicates a substantial probability for the Sr atom to move off the site center about 0.3 Å to one of four crystallographically equivalent positions (e.g.,  $\frac{1}{4}, 0.53, 0$ ).<sup>14</sup> From the ADP and nuclear density data alone, it is impossible to determine if this corresponds to a static displacement of the Sr atoms or to some dynamic motion between the four off-center sites and the center of the cage. Recent low-temperature ultrasonic attenuation measurements (0.3–10 K) on a  $\text{Sr}_8\text{Ga}_{16}\text{Ge}_{30}$  single crystal<sup>24</sup> provided direct evidence of a relatively high concentration of tunneling states, a feature normally associated with bulk glasses like  $\text{SiO}_2$ . These states are most likely associated with the ability of the Sr atoms to tunnel among the four sites. From the temperature dependence of the ADP data (slope), an Einstein temperature of 80 K is estimated. This value is substantially higher than the value of 53 K extracted from low-temperature heat-capacity data, and 46 K estimated from the lowest Raman mode frequency.<sup>25</sup> These disparate values indicate that it is not appropriate to analyze the Sr ADP data using an isolated harmonic oscillator. This does not mean, however, that there is not a characteristic Einstein mode associated with the Sr motion, only that this value cannot be determined from the ADP data in any simple analysis.

The Eu nuclear density distribution (Fig. 3) clearly shows the tendency of the Eu atoms to move away from the site center. Four separate peaks are resolved in the nuclear density maps, each approximately 0.4 Å from the center of the cage (0, 0.257, and 0.536). The Eu ADP data from this site are almost independent of temperature (Fig. 2), and hence no Einstein temperature can be determined from these data. The

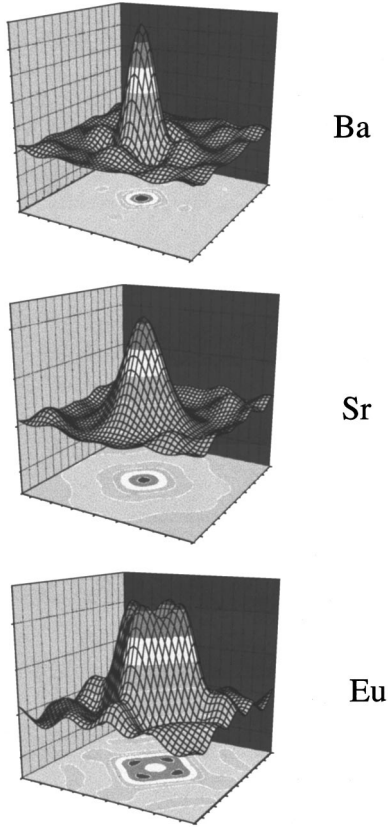


FIG. 3. Nuclear density at the Ba, Sr, or Eu site located at  $\frac{1}{4}, \frac{1}{2}$ , and 0 for  $\text{Ba}_8\text{Ga}_{16}\text{Ge}_{30}$  and  $\text{Sr}_8\text{Ga}_{16}\text{Ge}_{30}$  at 15 K and  $\text{Eu}_8\text{Ga}_{16}\text{Ge}_{30}$  at 40 K (above  $T_c$ ) in difference Fourier maps determined from single-crystal neutron-diffraction data. This site corresponds to the center of a large cage composed of 24 atoms of Ge or Ga (see Fig. 1). The amplitude along the vertical direction is proportional to the probability of finding the nucleus at a particular position. For all three figures, the area in the  $x$ - $y$  plane is  $1.5 \times 1.5 \text{ \AA}^2$ . It is likely that the Sr and Eu atoms can tunnel among the four nearby sites that are located between 0.3 and 0.5  $\text{Å}$  from the cage center.

increase in the Eu ADP values below 40 K (Fig. 2) is primarily due to additional magnetic scattering from a ferromagnetic alignment of the Eu magnetic moments which has not been accounted for in these ADP data. Low-temperature heat-capacity data suggest an Einstein temperature of about 30 K, a value in good agreement with the lowest Raman mode frequency of 33 K.<sup>25</sup> Low-temperature ultrasonic attenuation and elastic constant measurements on crystals of  $\text{Eu}_8\text{Ga}_{16}\text{Ge}_{30}$  are in progress.

### B. Magnetic measurements

Magnetic susceptibility and magnetization measurements were made on a single-crystal bar of  $\text{Eu}_8\text{Ga}_{16}\text{Ge}_{30}$  from 5 to 300 K in applied fields between 0.001 and 4 T. The magnetic susceptibility data between 75 and 300 K (Fig. 4) are accurately described by a Curie-Weiss law with an effective magnetic moment of  $8.1\mu_B$  which is about 2% larger than the  $\text{Eu}^{+2}$  free ion value of  $7.93\mu_B$  ( $\mu_B$  is the Bohr magneton). The Curie temperatures obtained from Curie-Weiss fits to the susceptibility data taken at 0.1 and 4 T are 35.7 and 34.5 K,

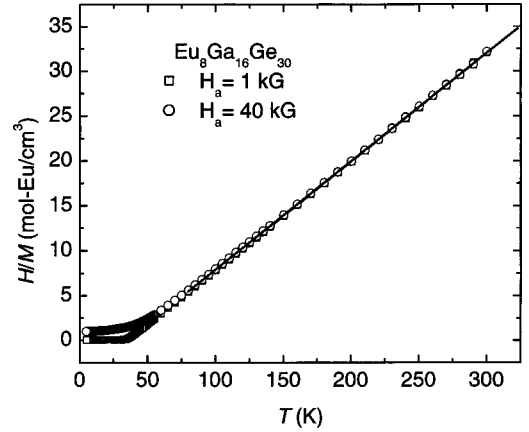


FIG. 4. Inverse magnetic susceptibility ( $H/M$ ) vs temperature for a  $\text{Eu}_8\text{Ga}_{16}\text{Ge}_{30}$  single crystal measured in fields of 0.1 and 4 T. Curie-Weiss fits to the data from 80 to 300 K indicate an effective magnetic moment of  $8.13\mu_B$  per Eu ion, and Curie-Weiss temperatures of 35.7 and 34.5 K, respectively. The measured effective moment is about 2% larger than the  $\text{Eu}^{+2}$  free-ion value of  $7.94\mu_B$  i.e.,  $g[J(J+1)]^{1/2}$ .

respectively, which suggests the onset of ferromagnetic ordering at about 35 K. This conclusion is verified by low temperature magnetization data (Fig. 5). Below  $T_c$ , the spontaneous magnetization is expected to decrease to zero as  $T_c$  is approached as  $(T_c - T)^\beta$ , where  $\beta$  is typically between 0.33 and 0.37.<sup>26</sup> Analysis of the low-field magnetization data assuming this power law gives a Curie temperature of 33 K. The saturation magnetization corresponds to a magnetic moment per Eu ion of  $7\mu_B$  (the free-ion value). The lack of any significant hysteresis in the magnetization upon cycling the magnetic field between 0 and 6 T at temperatures below 35 K implies that  $\text{Eu}_8\text{Ga}_{16}\text{Ge}_{30}$  is a soft ferromagnet with a very small coercive field of order 1–10 G. This is not unusual for an  $s$ -state ion. Single-crystal neutron structure refinement measurements at 12 K also show ferromagnetic order, and indicate that in zero applied magnetic field the magnetization is directed along the (100) direction. The soft ferromagnetism of  $\text{Eu}_8\text{Ga}_{16}\text{Ge}_{30}$  is similar to that observed for the filled skutterudite  $\text{EuFe}_4\text{Sb}_{12}$  which has a higher ordering temperature of 100 K.<sup>27</sup>

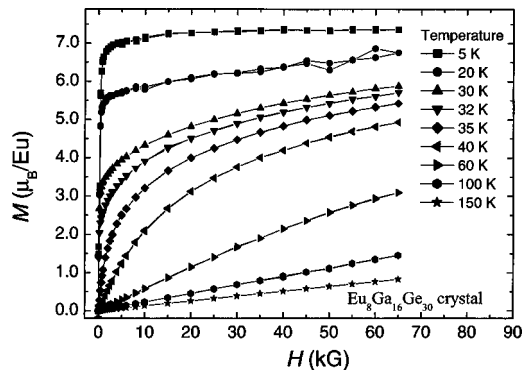


FIG. 5. Magnetization vs applied magnetic field for temperatures between 5 and 150 K. The saturation magnetization is near the free ion value of  $7\mu_B$  per Eu ion (i.e.,  $gJ$ ).

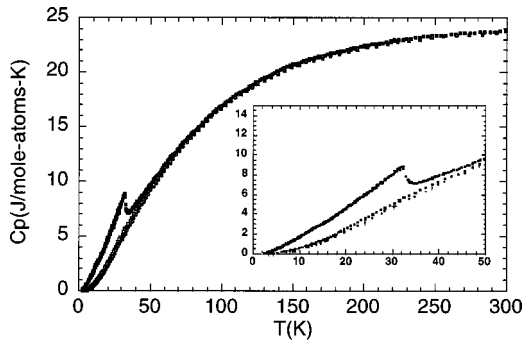


FIG. 6. Heat capacity vs temperature for  $\text{Eu}_8\text{Ga}_{16}\text{Ge}_{30}$ ,  $\text{Sr}_8\text{Ga}_{16}\text{Ge}_{30}$ , and  $\text{Ba}_8\text{Ga}_{16}\text{Ge}_{30}$  single crystals from 2 to 300 K in zero applied magnetic field. Above 80 K, the data from the three crystals are the same within  $\pm 1\%$ . The inset shows only the low temperature data from the three samples (top curve: Eu data; middle curve: Sr data; lower curve: Ba data).

The large separation distance between neighboring  $\text{Eu}^{+2}$  ions in the  $\text{Eu}_8\text{Ga}_{16}\text{Ge}_{30}$  structure (about 5.4 Å), and the poor bonding between the  $\text{Eu}^{+2}$  ions and Ga and Ge atoms forming the cage, suggests that the magnetic order in this material occurs via a Rudermann-Kittel-Kasuya-Yoshida (RKKY) indirect exchange interaction.<sup>28,29</sup> In the RKKY interaction, the Eu magnetic moments are coupled together through the conduction-electron spins. An interesting feature of this interaction is that it oscillates in sign (i.e., ferromagnetic or antiferromagnetic) as a function of distance from an Eu atom with a magnitude and period that depends on the conduction electron density. At low carrier densities, the Eu moments can only order via direct dipole-dipole interactions which is weak (ordering temperatures obtained via this mechanism are typically less than 1 K). Since  $\text{Eu}_8\text{Ga}_{16}\text{Ge}_{30}$  is a semiconductor, it should be possible to change the ordering temperature and perhaps the type of magnetic order by varying the carrier concentration. Initial attempts to change the carrier concentration in this compound significantly have not been successful, partially because of the close proximity of another cubic clathrate crystal structure mentioned in Sec. II A.

### C. Heat capacity

Heat-capacity measurements were made on  $\text{Eu}_8\text{Ga}_{16}\text{Ge}_{30}$ ,  $\text{Sr}_8\text{Ga}_{16}\text{Ge}_{30}$ , and  $\text{Ba}_8\text{Ga}_{16}\text{Ge}_{30}$  single crystals from 2 to 300 K in magnetic fields from 0 to 8 T. The zero-field heat capacity data for all three compounds are shown in Fig. 6. Above 80 K, the heat-capacity data are the same within the experimental error of 1%, and well described by a Debye heat capacity with a Debye temperature of about 300 K. The magnetic contribution to the Eu clathrate heat capacity,  $C_m$ , is estimated by subtracting the Ba clathrate data from that of the Eu. This difference is shown in Fig. 7 for applied magnetic fields of 0 and 8 T. In zero magnetic field the jump in  $C_m$  at  $T_c = 35$  K is about 24 J/K mole Eu, which is comparable to a value of 20.1 J/K mole Eu that is expected from mean-field theory for magnetic moments with a spin of  $\frac{7}{2}$ .<sup>30</sup> Mean-field theory, however, is not expected to accurately describe the zero-field magnetic contribution of the heat capacity of any real material because of a number of unrealistic

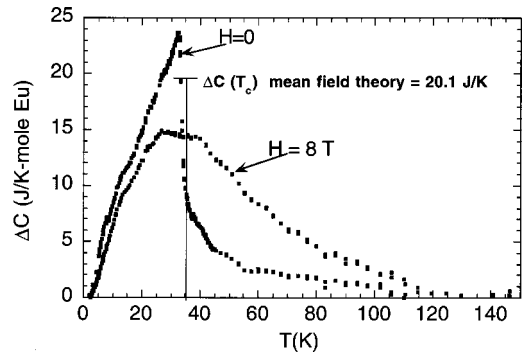


FIG. 7. Magnetic contribution to the heat capacity determined by subtracting the  $\text{Ba}_8\text{Ga}_{16}\text{Ge}_{30}$  heat-capacity data from that of  $\text{Eu}_8\text{Ga}_{16}\text{Ge}_{30}$ . Note that in this figure the heat capacity is given per mole of Eu atoms, whereas in the previous figure it was given per mole of atoms.

simplifications. For example, above  $T_c$ , magnetic fluctuations that significantly contribute to  $C_m$  are not treated in a mean-field picture of the phase transition, and at low temperatures spin waves are not considered. The magnetic heat capacity at 8 T is significantly broadened in temperature. This is not surprising, since each Eu ion has a magnetic moment of  $7\mu_B$ , which in a field of 8 T corresponds to an effective temperature of 40 K ( $7\mu_B H/k_B$ ).

The magnetic entropy that is removed from the Eu spin system during the transition from free paramagnetic spins to the ferromagnetic ground state should be equal to  $R \ln(2J+1) = R \ln 8 = 17.28$  J/K mole Eu. The magnetic entropy can be determined experimentally by integrating  $C_m/T$  from 0 to about 150 K using the data shown in Fig. 7. This results in a calculated entropy of about 28 J/K mole Eu, which is significantly larger than  $R \ln 8$ . Initially we thought that this additional entropy (about  $R \ln 4$ ) might be associated with a freezing out of the motion of the Eu atoms among the four sites (see Fig. 3). This analysis, however, is not correct. Although the heat-capacity data from the three clathrates are virtually identical above 80 K, at low temperatures (5–30 K) the low-energy Einstein modes are significantly different. Below about 30 K, the Ba clathrate heat-capacity data are not a good reference for the lattice heat capacity of the Eu clathrate. From fits to the low-temperature heat-capacity data, we estimate the characteristic Einstein temperatures for Ba, Sr, and Eu atoms to be 60, 53, and 30 K, respectively. These values agree well with Raman data from the Sr and Eu clathrates, which give low-energy modes at 46 and 33 K, respectively,<sup>25</sup> as well as with detailed lattice-dynamics calculations.<sup>18</sup> The difference in entropy between Einstein oscillators with Einstein temperatures of 60 and 30 K is about  $R \ln 4$ , which accounts for the apparent excess in the magnetic entropy from the data in Fig. 7.

### D. Thermal conductivity

The lattice thermal conductivity of single crystals of  $\text{Eu}_8\text{Ga}_{16}\text{Ge}_{30}$ ,  $\text{Sr}_8\text{Ga}_{16}\text{Ge}_{30}$ , and  $\text{Ba}_8\text{Ga}_{16}\text{Ge}_{30}$  from 2 to 300 K are displayed in Fig. 8 in both linear and (inset)  $\log T$  vs

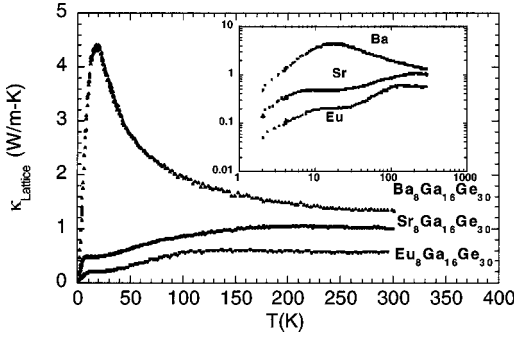


FIG. 8. Lattice thermal conductivity vs temperature for  $\text{Eu}_8\text{Ga}_{16}\text{Ge}_{30}$ ,  $\text{Sr}_8\text{Ga}_{16}\text{Ge}_{30}$ , and  $\text{Ba}_8\text{Ga}_{16}\text{Ge}_{30}$  single crystals. Inset shows same data displayed as  $\log \kappa_{\text{lattice}}$  vs  $\log T$ . Application of a magnetic field of 8 T had no significant effect on the thermal conductivity data ( $\leq \pm 2\%$ ).

$\log \kappa_{\text{lattice}}$  plots. The linear plots are more relevant for applications, while the log-log plots are traditionally used in discussing phonon scattering mechanisms. The lattice thermal conductivity was estimated from the total thermal conductivity data using the Wiedemann-Franz approximation and the resistivity data shown in Fig. 9. The lattice thermal conductivity data from the Eu and Sr clathrates are similar to that reported previously on polycrystalline samples<sup>8,9,12</sup> although no clear “resonant dip”<sup>12</sup> was seen in any of our samples; only a broad plateau in the 10–20-K temperature range. It is possible that electron-phonon scattering from the high carrier concentrations in our crystals ( $\approx 1 \times 10^{21}$  electrons/cm<sup>3</sup>) washes out a “resonant dip.”

The thermal conductivity of glasses,  $\kappa$ , is not only very small,<sup>6,7</sup> but also displays a universal temperature dependence:  $\kappa$  varies as  $T^2$  below 1 K, has a plateau in the region from 10 to 20 K, and is roughly independent of temperature above 100 K. This behavior is qualitatively different from ordinary crystalline behavior, in which  $\kappa$  reaches a maximum between 20 and 50 K and shows no plateau. The difference between crystalline and glasslike behavior is illustrated in Fig. 8. The Eu and Sr clathrates show a typical glasslike thermal conductivity. Although the present data do not extend below 2 K, previous thermal conductivity measurements<sup>9</sup> on  $\text{Sr}_8\text{Ga}_{16}\text{Ge}_{30}$  below 1 K showed approximately a  $T^2$  temperature dependence, and tunneling states were measured using ultrasonic attenuation measurements.<sup>24</sup>

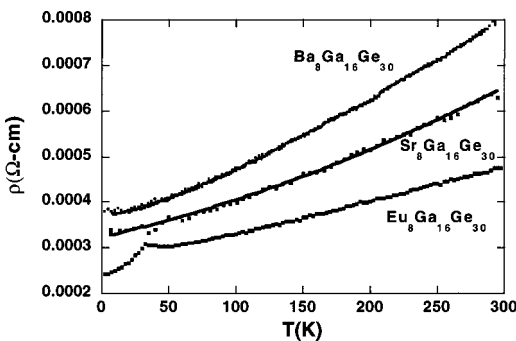


FIG. 9. Resistivity vs temperature for three single-crystal samples.

The lattice thermal conductivity of the Ba clathrate is low, and is about the same as that for vitreous silica (1.3 W/m K) at room temperature. This low value is partially due to the rattling of the Ba atoms, which effectively scatter the acoustic phonons that carry most of the heat. The temperature dependence of the lattice thermal conductivity of  $\text{Ba}_8\text{Ga}_{16}\text{Ge}_{30}$ , however, is like that of a normal crystalline solid.

The lattice thermal conductivity of all three compounds was measured in a magnetic field of 8 T. Within experimental error ( $\pm 3\%$ ), the field had no effect on heat transport in these materials. This result was surprising for the Eu clathrate, since in this compound the Eu rattlers clearly have a large effect on the lattice thermal conductivity in zero field. This null result may imply a small spin coupling to the acoustic phonons.

We have suggested previously<sup>24</sup> that both “rattling” and “tunneling” states appear to be necessary to produce a true glasslike thermal conductivity in these clathrate single crystals. As noted previously,<sup>25,31</sup> single crystals with well-defined defects or localized modes are the best materials on which to study the origin and effects of tunneling states on the low-temperature properties of solids. The semiconducting clathrate crystals may prove to be ideal systems for quantitative studies of specific structural features that produce tunneling states. The nuclear density data shown in Fig. 3 may be regarded as a “snapshot” of the tunneling states in the Sr and Eu clathrate crystals. Interesting recent work in Ref. 31 provided additional insight into the origin of tunneling states and the glasslike thermal conductivity. These authors found that if amorphous silicon is hydrogenated, the low-temperature tunneling states associated with glasses disappear—even though the solid is structurally amorphous. These data clearly show the importance of understanding which specific structural features actually result in a glasslike thermal conductivity.

### E. Electrical transport

The electrical resistivities of  $\text{Eu}_8\text{Ga}_{16}\text{Ge}_{30}$ ,  $\text{Sr}_8\text{Ga}_{16}\text{Ge}_{30}$ , and  $\text{Ba}_8\text{Ga}_{16}\text{Ge}_{30}$  were measured from 2 to 300 K in various magnetic fields from 0 to 8 T. The zero-field resistivity data are shown in Fig. 9 for three single crystals. The resistivity data from the Sr and Ba crystals are typical of heavily doped semiconductors. The  $\text{Eu}_8\text{Ga}_{16}\text{Ge}_{30}$  resistivity data show the effects of the ferromagnetic phase transition below about 40 K. The rapid drop in the resistivity for temperatures less than 35 K is characteristic of the loss of spin disorder scattering that occurs below the magnetic ordering temperature.<sup>32,33</sup> For temperatures less than 34 K, the resistivity is approximately proportional to  $T^2$ , although we do not attach any theoretical significance to this observation. The magnetoresistance of all three compounds was investigated. Only for a Eu clathrate near its Curie temperature (Fig. 10) was the magnetoresistance significant, amounting to about a 10% decrease in resistance with an applied field of 8 T. A magnetoresistance of this magnitude near  $T_c$  is consistent with the suppression of spin-disorder scattering due to the increased magnetization

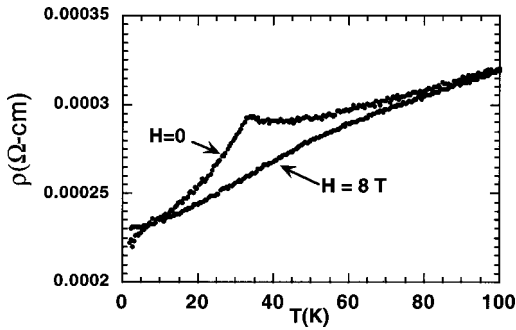


FIG. 10. Resistivity vs temperature of  $\text{Eu}_8\text{Ga}_{16}\text{Ge}_{30}$  in magnetic fields of 0 and 8 T.

of the sample in a large field.<sup>32,33</sup> The magnitude of the spin-disorder resistivity in the present sample is about  $30 \mu\Omega \text{ cm}$ .

The Seebeck coefficient versus temperature is shown for all three crystals in Fig. 11. The room-temperature values of  $50\text{--}55 \mu\text{V/K}$  are typical for heavily doped semiconductors. The measured room-temperature carrier concentrations for the crystals are  $\approx 10^{21} \text{ electrons/cm}^3$ , which implies electron mobilities of  $10\text{--}15 \text{ cm}^2/\text{V s}$ . These values are similar to those previously reported,<sup>9,13</sup> and are reasonably high for such heavy doping. The Hall mobility of the carriers increases with decreasing temperature, which would suggest that the scattering of the carriers is dominated by acoustic phonons. A more detailed analysis of the scattering mechanisms, however, would be more appropriate for crystals with much lower carrier concentrations, which to date we have not been able to grow. Assuming a single parabolic band and scattering by acoustic phonons implies an electron effective mass of  $3m_0$ , where  $m_0$  is the free-electron mass. This relatively high effective mass suggests that the conduction band may be degenerate (multivalleyed).<sup>4</sup>

#### F. Superconductivity

Previous work<sup>34</sup> reported superconductivity at  $7.5 \pm 0.5 \text{ K}$  in a polycrystalline sample of  $\text{Ba}_8\text{Ga}_{16}\text{Ge}_{30}$ . Motivated by this report, we carefully examined two single crystals of  $\text{Ba}_8\text{Ga}_{16}\text{Ge}_{30}$  for any evidence of superconductivity using heat capacity, resistivity, and ac susceptibility measurements. For temperatures above 2 K, we did not observe any evidence of superconductivity in the single crystals. It is possible that the carrier concentration in our crystals was too

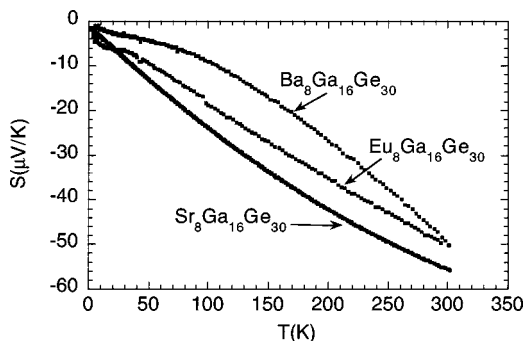


FIG. 11. Seebeck coefficient vs temperature.

low to result in superconductivity, although the carrier concentrations were high for a semiconductor ( $\approx 10^{21} \text{ electrons/cm}^3$ ). A more likely explanation is that the samples studied previously had small amounts of an impurity phase such as Ga or  $\text{BaGe}_2$ —both of which can be superconducting in the  $1\text{--}8\text{-K}$  temperature range.<sup>35,36</sup>

#### IV. SUMMARY AND CONCLUSIONS

Large single crystals of  $\text{Eu}_8\text{Ga}_{16}\text{Ge}_{30}$ ,  $\text{Sr}_8\text{Ga}_{16}\text{Ge}_{30}$ , and  $\text{Ba}_8\text{Ga}_{16}\text{Ge}_{30}$  have been grown. The Ba, Sr, and Eu atoms at the  $6d$  site  $(\frac{1}{4}, \frac{1}{2}, 0)$  in this structure exhibited large ADPs indicating a large mean-square displacement of each atom type about its equilibrium position (Fig. 2). The Ba ADP data could be analyzed using an Einstein oscillator model to describe the Ba motion, but for the Sr and Eu atoms the ADP data were further complicated by the ability of the Sr and Eu atoms to move away from the center of the cage ( $1/4, 1/2$ , and 0 positions) to one of four nearby positions (Fig. 3). In this situation it is not clear how to extract characteristic Einstein temperatures from the ADP data. Low-temperature heat-capacity measurements, however, indicated approximate Einstein temperatures of 60, 53, and 30 K for the Ba, Sr, and Eu atoms, respectively.

The electrical transport data from the three crystals are similar. All three compounds have similar carrier concentrations ( $\approx 10^{21} \text{ cm}^{-3}$ ), mobilities ( $10\text{--}15 \text{ cm}^2/\text{V s}$ ), and carrier effective masses ( $\approx 3m_e$ ). Preliminary Hall measurements indicate that the mobility increases with decreasing temperature, a feature consistent with the scattering of carriers by acoustic phonons.

There is a striking difference, however, between the lattice thermal conductivity of the Ba clathrate and the lattice thermal conductivity of the Sr and Eu clathrates. The lattice thermal conductivities of the Eu and Sr clathrates are similar to that of a bulk oxide glass like  $\text{SiO}_2$  (Fig. 8). The room-temperature lattice thermal conductivity of the Ba clathrate is low ( $1.3 \text{ W/m K}$ ) which is about the same as the room temperature value for vitreous silica. The temperature dependence, however, is much like a normal crystalline solid (Fig. 8). It is suggested that, at least for this family of compounds, both *rattling and tunneling states* are necessary to produce a true glasslike thermal conductivity. The nuclear density maps shown in Fig. 3 may, in fact, represent a “shapshot” of tunneling states in the Eu and Sr clathrate crystals.

Magnetic measurements on a  $\text{Eu}_8\text{Ga}_{16}\text{Ge}_{30}$  single crystal showed ferromagnetic order with a Curie temperature of 33 K and an easy direction for Eu spins along the (100) direction (Figs. 4 and 5). Very little hysteresis was found during either temperature or magnetic-field sweeps, implying a very small coercive field of the order of  $1\text{--}10 \text{ G}$ . The weak bonding and large separation distance between Eu spins suggest that magnetic ordering occurs via a RKKY interaction.

$\text{Eu}_8\text{Ga}_{16}\text{Ge}_{30}$  exhibited a negative magnetoresistance of 10% near  $T_c$  in a field of 8 T. This result is consistent with the suppression of spin-disorder scattering due to the increased magnetization of the sample in an applied magnetic field. No superconductivity was detected in heavily doped  $\text{Ba}_8\text{Ga}_{16}\text{Ge}_{30}$  single crystals at temperatures above 2 K. An-

nealing polycrystalline  $\text{Eu}_8\text{Ga}_{16}\text{Ga}_{30}$  samples in a dynamic vacuum resulted in a phase with a completely different crystal structure. This structure is isomorphic with another cubic clathrate phase,  $\text{Ba}_8\text{Ga}_{16}\text{Sn}_{30}$  first reported in Ref. 10. The  $\text{Eu}_8\text{Ga}_{16}\text{Ga}_{30}$  clathrate phase has the space group of  $I-43m$  (No. 217) and a lattice constant of 10.62 Å. The properties of this phase will be reported elsewhere.

## ACKNOWLEDGMENTS

It is a pleasure to acknowledge useful discussions with V. Keppens, G. Nolas, and N. Dilley, and the technical assistance of J. Kolopus and L. Zevenbergen. Oak Ridge National Laboratory is managed by UT-Battelle, LLC, for the U.S. Department of Energy under Contract No. DE-AC05-00OR22725.

- <sup>1</sup>G. A. Slack, in *CRC Handbook of Thermoelectrics*, edited by D. M. Rowe (Chemical Rubber, Boca Raton, FL, 1995), Chap. 34, p. 407.
- <sup>2</sup>B. C. Sales, D. Mandrus, and R. K. Williams, *Science* **272**, 1325 (1996).
- <sup>3</sup>J.-P. Fleurial, A. Borshchevsky, T. Caillat, D. T. Morelli, and G. P. Meisner, in *Proceedings of the Fifteenth International Conference on Thermoelectrics Pasadena CA* (IEEE, Piscataway, NJ, 1996), p. 91.
- <sup>4</sup>B. C. Sales, D. Mandrus, B. C. Chakoumakos, V. Keppens, and J. R. Thompson, *Phys. Rev. B* **56**, 15 081 (1997).
- <sup>5</sup>D. T. Morelli and G. P. Meisner, *J. Appl. Phys.* **77**, 3777 (1995).
- <sup>6</sup>R. C. Zeller and R. O. Pohl, *Phys. Rev. B* **4**, 2029 (1971).
- <sup>7</sup>*Amorphous Solids: Low Temperature Properties*, edited by W. A. Phillips (Springer-Verlag, Berlin, 1981).
- <sup>8</sup>G. S. Nolas, J. L. Cohn, G. A. Slack, and S. B. Schujman, *Appl. Phys. Lett.* **73**, 178 (1998).
- <sup>9</sup>J. L. Cohn, G. S. Nolas, V. Fessatidis, T. H. Metcalf, and G. A. Slack, *Phys. Rev. Lett.* **82**, 779 (1999).
- <sup>10</sup>B. Eisenmann, H. Schafer, and R. Zagler, *J. Less-Common Met.* **118**, 43 (1986).
- <sup>11</sup>B. Kuhl, A. Czybulka, and H-U. Schuster, *Z. Anorg. Allg. Chem.* **621**, 1 (1998).
- <sup>12</sup>G. S. Nolas, T. J. R. Weakley, and J. L. Cohn, *Chem. Mater.* **11**, 2470 (1999).
- <sup>13</sup>V. L. Kuznetsov, L. A. Kuznetsov, A. E. Kaliazin, and D. M. Rowe, *J. Appl. Phys.* **87**, 7871 (2000).
- <sup>14</sup>B. C. Chakoumakos, B. C. Sales, D. Mandrus, and G. S. Nolas, *J. Alloys Compd.* **296**, 80 (2000).
- <sup>15</sup>G. S. Nolas, T. J. R. Weakley, J. L. Cohn, and R. Sharma, *Phys. Rev. B* **61**, 3845 (2000).
- <sup>16</sup>J. D. Corbett, *Chem. Rev.* **85**, 383 (1985).
- <sup>17</sup>N. P. Blake, L. Mollnitz, G. D. Stucky, H. Metiu, in *Proceedings of the 18th International Conference on Thermoelectrics, ICT99, Baltimore, MD 1999* (IEEE, Piscataway, NJ, 1999), p. 489.
- <sup>18</sup>J. Dong, O. F. Sankey, G. K. Ramachandran, and R. F. McMillan, *J. Appl. Phys.* **87**, 7726 (2000).
- <sup>19</sup>B. C. Sales, B. C. Chakoumakos, D. Mandrus, and J. W. Sharp, *J. Solid State Chem.* **146**, 528 (1999).
- <sup>20</sup>B. C. Sales, D. Mandrus, and B. C. Chakoumakos, *Recent Trends in Thermoelectric Materials Research II*, Semiconductors and Semimetals Vol 70, edited by T. M. Tritt (Academic, San Diego, 2001), Chap. 1, pp. 1–34.
- <sup>21</sup>B. C. Sales, B. C. Chakoumakos, and D. Mandrus, *Phys. Rev. B* **61**, 2475 (2000).
- <sup>22</sup>J. W. Sharp, B. C. Sales, D. Mandrus, and B. C. Chakoumakos, *Appl. Phys. Lett.* **74**, 3794 (1999).
- <sup>23</sup>B. C. Sales, B. C. Chakoumakos, D. Mandrus, J. W. Sharp, N. R. Dilley, and M. B. Maple, in *Thermoelectric Materials 1998—The Next Generation Materials for Small-Scale Refrigeration and Power Generation Applications*, edited by T. M. Tritt, M. G. Kanatzidis, G. D. Mahan, and H. B. Lyon Jr. (Materials Research Society, Warrendale, PA, 1998), p. 13.
- <sup>24</sup>V. Keppens, B. C. Sales, D. Mandrus, B. C. Chakoumakos, and C. Laermans, *Philos. Mag. Lett.* **80**, 807 (2000).
- <sup>25</sup>G. S. Nolas and C. A. Kendziora, *Phys. Rev. B* **62**, 7157 (2000).
- <sup>26</sup>N. W. Ashcroft and N. D. Mermin, *Solid State Physics* (Holt, Rinehart and Winston, New York, 1976), p. 699.
- <sup>27</sup>M. E. Dannebrock, C. B. H. Evers, and W. Jeitschko, *J. Phys. Chem. Solids* **57**, 381 (1996).
- <sup>28</sup>P. Fazekas, *Lecture Notes on Electron Correlation and Magnetism* (World Scientific, Singapore, 1999), p. 643.
- <sup>29</sup>R. J. Elliot, in *Magnetism*, edited by G. T. Rado and H. Suhl (Academic Press, New York, 1965), Vol. II A, Chap. 7.
- <sup>30</sup>D. C. Mattis, *Theory of Magnetism* (Harper and Row, New York, 1965), p. 232.
- <sup>31</sup>R. O. Pohl, X. Liu, and R. S. Crandall, *Curr. Opin. Solid State Mater. Sci.* **3**, 281 (1999).
- <sup>32</sup>K. W. McEwen, in *Handbook on the Chemistry and Physics of Rare Earths*, edited by K. A. Gschneidner and L. Eyring (North-Holland, New York, 1978), Vol. I, Chap. 6, p. 470.
- <sup>33</sup>P. G. DeGennes and J. Freidel, *J. Phys. Chem. Solids* **4**, 71 (1958).
- <sup>34</sup>J. D. Bryan, V. I. Sardanov, G. D. Stucky, and D. Schmidt, *Phys. Rev. B* **60**, 3064 (1999).
- <sup>35</sup>J. Evers, G. Oehlinger, and H. R. Ott, *J. Less-Common Met.* **69**, 389 (1980).
- <sup>36</sup>*CRC Handbook of Chemistry and Physics*, 61st ed. (CRC Press, Boca Raton, FL, 1980), p. E-89.